International Journal of Research
Available at https://edupediapublications.org/journals
e-ISSN: 2348-6848
p-ISSN: 2348-795X
Volume 04 Issue-17
December 2017

Design and Analysis of Quasi-Z-Source Four-Leg Inverter with Model Predictive Control of Pv System

E Sharadha & D Aravind
[1]M.Tech(student), St. Martin's Engineering College, Dhullapally, Secunderabad, Telangana.
[2]Assistant Professor, St. Martin's Engineering College, Dhullapally, Secunderabad, Telangana.

ABSTRACT-*This paper presents a model predictive control (MPC) scheme with pv system using quasi-Z-source (qZS) three-phase four leg inverter. Photovoltaics (PV) is a term which covers the conversion of light into electricity using semiconducting materials that exhibit the photovoltaic effect, a phenomenon studied in physics, photochemistry, and electrochemistry. In order to cope with the drawbacks of traditional voltage source inverters (VSIs), a qZS three-phase four-leg inverter topology is proposed. This topology features a wide range of voltage gain which is suitable for applications in renewable energy-based power systems, where the output of the renewable energy sources varies widely with operating conditions such as wind speed, temperature, and solar irradiation. To improve the capability of the controller, an MPC scheme is used which implements a discrete-time model of the system. The controller handles each phase current independently, which adds flexibility to the system. Simulation and experimental studies verify the performances of the proposed control strategy under balanced and unbalanced load conditions as well as single-phase open-circuit fault condition.*

Index Terms—DC–AC power conversion, four-leg inverter, model predictive control (MPC), PV system, quasi-Z-source inverter (qZSI)

INTRODUCTION

Photovoltaic (PV) power generation is becoming more promising since the introduction of the thin film PV technology due to its lower cost, excellent high temperature performance, low weight, flexibility, and glass-free easy installation. The performance of these renewable energy systems thus depends on the power converter topology and control method [1].

The dc/dc boost converter is often used as an input stage to create a well-regulated voltage for the VSI. However, this solution results in complex power circuit and multiloop control structure which leads to lower reliability and higher cost.

The CSI has some drawbacks as follows. 1) Its output voltage cannot be lower than the dc input voltage. 2) Overlap time between phase legs is required to avoid the open circuit of all upper switching devices or all lower devices. Otherwise, an open circuit of the dc inductor would occur and destroy the devices.

They advantageously utilize the shoot-through of the inverter bridge to boost voltage in the VSI (or open circuit in the CSI to buck voltage). Thus, buck–boost functionality is achieved with a single-stage power conversion with a simple L–C network [7]. The model predictive control (MPC) is an attractive alternative to the classical control methods due to its fast dynamic response, simple concept, and ability to include different nonlinearities and constraints [22]. The major advantage of MPC lies in the direct application of the control action to the converter, without requiring a modulation stage. Solar PV has specific advantages as an energy source: its operation generates no pollution and no greenhouse gas emissions once installed, it shows simple scalability in respect of power needs and silicon has large availability in the Earth's crust.

This paper presents MPC strategy of quasi-Z-source (qZS) three-phase four-leg inverter. As a response to the gaps in this research area, the contributions of this study are summarized as follows.

1) qZS network has been used instead of a dc–dc+dc–ac converter to overcome the drawbacks of traditional three phase VSI topology and two-stage power conversion.
2) A three-phase four-leg inverter has been employed to ensure reliable operation of renewable energy-based power generation system under balanced and unbalanced load conditions.
3) MPC is used to control load current and qZS network capacitor voltage with high accuracy and fast response.

A photovoltaic system, also PV system or solar power system, is a power system designed to supply usable solar power by means of photovoltaics. It consists of an arrangement of several components, including solar panels to absorb and convert sunlight into electricity, a solar inverter to change the electric current from DC to AC, and mounting cabling and other electrical accessories to set up a working system.

III QZS FOUR LEG INVERTER MODEL

Topology

The qZS four-leg inverter topology with R–L output filter is shown in Fig. 1. This topology can

International Journal of Research
Available at https://edupediapublications.org/journals
e-ISSN: 2348-6848
p-ISSN: 2348-795X
Volume 04 Issue-17
December 2017

be investigated as two stages: 1) the qZS network and 2) four-leg inverter with R–L output filter and load

In the first stage of this topology, the qZS is made of an L–C impedance network, which can boost the dc voltage in response to the so-called shoot-through zero state of the inverter switching cycle. In the shoot-through zero state, two semiconductor switches in the same leg are simultaneously switched on to create short-circuit across the dc link. During this state, energy is transferred in the qZS network from the capacitors to the inductors, and this state is used to boost the dc voltage.

In the second stage of this topology, the four-leg inverter is used.

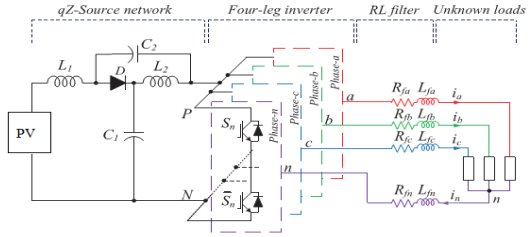

Fig. 1. qZS three-phase four-leg inverter topology.

As shown in Fig. 1, the load neutral point is connected to the mid-point of the inverter's fourth phase leg to allow for zero sequence current/voltage. However, the addition of an extra leg makes the switching schemes more complicated compared to a three-leg VSI. Nevertheless, using the extra phase leg improves inverter capability and reliability. The four-leg inverter can be used under balanced/unbalanced and/or linear/nonlinear load conditions.

Mathematical Model of the qzs Network

The equivalent circuits of the qZS network in non-shoot through and shoot-through states are illustrated in Fig. 2(a) and (b), respectively [33].

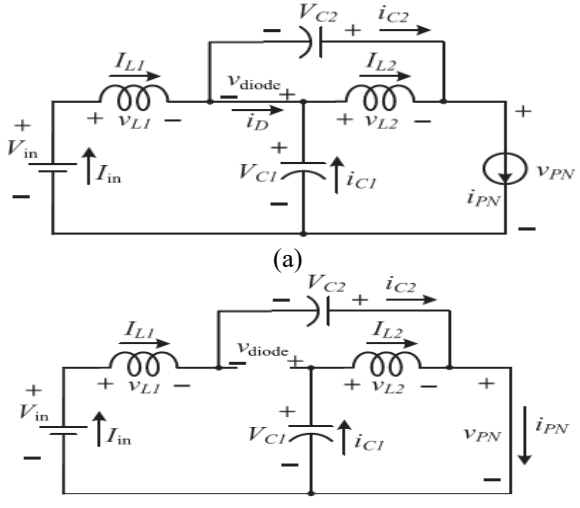

(a)

(b)

Fig. 2. Equivalent circuit of the qZS network. (a) In nonshoot-through state. (b) In shoot-through state.

All voltages and currents are defined in this figure and the polarities are shown with arrows.

Non shoot-through state

During the non shoot through state, four-leg inverter model is represented by a constant current source; it can be seen from Fig. 2(a). By applying Kirchhoff's voltage law to Fig. 2(a), inductor voltages (vL1 and vL2), dc-link voltage (vPN), and diode voltage (vdiode) are written as

$$V_{L1} = V_{in} - V_{C1}, V_{L2} = -V_{C2} \quad (1)$$

$$V_{PN} = V_{C1} - v_{L2} = V_{C1} + V_{C2}\ V_{diode} = 0 \quad (2)$$

Shoot-through state

During the shoot-through state, four-leg inverter model is represented by short-circuit, it can be seen from Fig. 2(b). By applying Kirchhoff's voltage law to Fig. 2(b), inductors voltages (vL1 and vL2), dc-link voltage (vPN), and diode voltage (vdiode) are written as

$$V_{L1} = V_{C2} + V_{in}, V_{L2} = V_{C1} \quad (3)$$

$$v_{PN} = 0, V_{diode} = V_{C1} + V_{C2} \quad (4)$$

At steady state, the average voltage of the capacitors over one switching cycle are

$$V_{C1} = \frac{T_1}{T_1 - T_0} V_{in}$$

$$V_{C2} = \frac{T_0}{T_1 - T_0} V_{in} \quad (5)$$

where T0 is the duration of the shoot-through state, T1 is the duration of the nonshoot-through state, and Vin is the input dc voltage.

From (2), (4), and (5), the peak dc-link voltage across the inverter bridge in Fig. 1 is

$$v_{PN} = V_{C1} + V_{C2} = \frac{T}{T_1 - T_0} V_{in} = BV_{in} \quad (6)$$

where T is the switching cycle (T0 + T1) and B is the boost factor of the qZSI. The average current of the inductors L1 and L2 can be calculated from the system power P

$$I_{L1} = I_{L2} = I_{in} = {}^{P}/_{V_{in}} \quad (7)$$

Applying Kirchhoff's current law and (7) results in

$$i_{C1} = i_{C2} = i_{PN} - I_{L1} \quad (8)$$

The voltage gain (G) of the qZSI can be expressed as

$$G = {}^{\hat{v}_{in}}/_{0.5vPN} = MB \quad (9)$$

where M is the modulation index and ˆvln is the peak ac-phase voltage.

Mathematical Model of the Four-Leg Inverter

The equivalent circuit of the four-leg inverter with the output R–L filter is shown in Fig. 3.

For a three-phase four-leg inverter, the addition of the fourth leg makes the switching states 16. The valid switching states with the corresponding

phase and line voltages for the traditional four-leg inverter are presented. In addition to these switching states, for this application, one extra switching state is required in order to ensure shoot-through state.

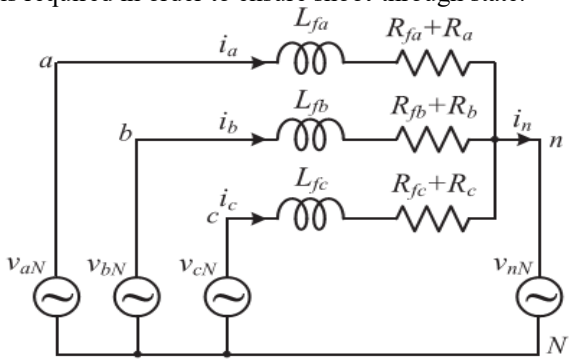

Fig. 3. Equivalent circuit of the three-phase four-leg inverter

Therefore, a total of 17 switching states are used in this application.

The voltage in each leg of the four-leg inverter can be expressed as

$$v_aN = S_a v_{dc}$$
$$v_bN = S_b v_{dc}$$
$$v_cN = S_c v_{dc}$$
$$v_nN = S_n v_{dc} \quad (10)$$

where Sa, Sb, Sc, and Sn are the switching states, and vdc and vnN are dc link and load neutral voltages, respectively.

The output voltage of this inverter can be written in terms of the previous inverter voltages

$$v_{an} = (S_a - S_n)v_{dc}$$
$$v_{bn} = (S_b - S_n)v_{dc}$$
$$v_{cn} = (S_c - S_n)v_{dc} \quad (11)$$

By applying Kirchhoff's voltage law to Fig. 3, the inverter voltages can be expressed in terms of load-neutral voltages and load currents as follows:

$$v_{aN} = (R_{fa} + R_a)i_a + L_{fa}\frac{di_a}{dt} + v_n\mathrm{N}$$
$$v_{bN} = (R_{fb} + R_b)i_b + L_{fb}\frac{di_b}{dt} + v_n\mathrm{N}$$
$$v_{cN} = (R_{fc} + R_c)i_c + L_{fc}\frac{di_c}{dt} + v_n\mathrm{N} \quad (12)$$

From (11) and (12), the output voltages can be expressed as

$$v_{aN} = (R_{fa} + R_a)i_a + L_{fa}\frac{di_a}{dt}$$
$$v_{bN} = (R_{fb} + R_b)i_b + L_{fb}\frac{di_b}{dt}$$
$$v_{cN} = (R_{fc} + R_c)i_c + L_{fc}\frac{di_c}{dt} \quad (13)$$

Which is simplified to

$$v_j = (R_{fj} + R_j)i_j + L_{fj}\frac{di_j}{dt}, \text{j=a,b,c} \quad (14)$$

and neutral current in can be written as

$$i_n = i_a + i_b + i_c \quad (15)$$

The expression for output current, derived from (14), is

$$\frac{di_j}{dt} = \frac{1}{L_f}(v_j - (R_{fj} + R_j)i_j), j = a, b, c \quad (16)$$

IV PROPOSED MPC

The proposed MPC scheme is shown in Fig. 4. It has two main layers: 1) a predictive model and 2) cost function optimization.

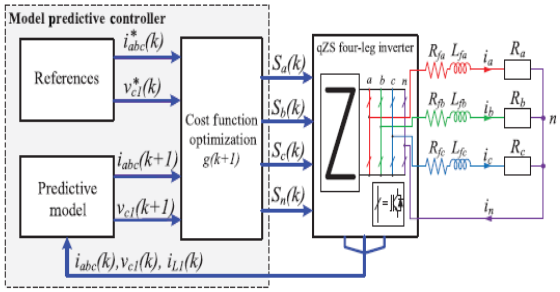

Fig. 4. Block diagram of the proposed MPC scheme.

The discrete-time model of the system is used to predict future behavior of the control variables. The cost function is used to minimize the error between the reference and the predicted control variables in the next sampling time. This control technique has several advantages as follows: easy to implement in both linear and nonlinear systems, it shows high accuracy and fast dynamic response, and it has very small steady-state error throughout different operating points. More detailed analysis of the MPC technique and its characteristics can be found in [35]

Here, the proposed MPC scheme is described in the following steps:

1) determination of references;
2) build discrete-time models of the system;
3) define a cost function g;
4) prepare control algorithm.

Determination of References

DC-link voltage and output currents references are normally obtained through maximum power point tracking algorithm for RESs. However, the objective of this paper is the control capability of the qZS four-leg inverter. For this reason, without loss of generality, these references are left to be defined by the user.

Discrete-Time Models of the System

The control of the qZS four-leg inverter output currents (ia, ib, ic) and capacitor voltage (VC1) required two discrete time models be created from the continuous-time equations. To do that, the general structure of the forward-difference Euler

International Journal of Research
Available at https://edupediapublications.org/journals
e-ISSN: 2348-6848
p-ISSN: 2348-795X
Volume 04 Issue-17
December 2017

equation (17) is used so as to compute the differential equations of the output current and the capacitor voltage

$$\frac{df}{dt} \approx \frac{f(x_0+h)-f(x_0)}{h} \quad (17)$$

To estimate the value in the next sample time, for a suitably small time step, (17) becomes the discretization equation

$$\frac{\Delta f(k)}{\Delta t} \approx \frac{f(k+1)-f(k)}{T_s} \quad (18)$$

Where Ts is sampling time.

Predictive Model I

This model is used to predict future behavior of each of the output currents (ia, ib, ic). The continuous-time expression for each phase current is given in (16). By substituting (18) into (16), the discrete-time model for each output phase current is

$$i_j(k+1) = A_v V_j(k+1) + A_i i_j(k), j = a, b, c \quad (19)$$

where ij(k + 1) is the predicted output current vector at the next sampling time and Av and Ai are constants as defined by

$$A_v = \frac{T_s}{L_f + (R + R_f)T_s}$$

$$A_i = \frac{L_f}{L_f + (R+R_f)T_s} \quad (20)$$

Predictive Model II

This model is used to predict future behavior of the capacitor voltage (VC1). The continuous time model of the capacitor current can be expressed as

$$i_{C1} = C_1 \frac{d(V_{C1} - i_{C1} r_c)}{dt} \quad (21)$$

where C1 and rc are the capacitance and the equivalent series resistance (ESR) of the capacitor, respectively. Based on (21), the capacitor voltage is derived as

$$\frac{dV_{C1}}{dt} = r_c \frac{di_{C1}}{dt} + \frac{1}{C_1} i_{C1} \quad (22)$$

By substituting (18) into (22), the discrete-time model of the VC1 can be obtained as

$$V_{C1}(k+1) = V_{C1}(k) + i_{C1}(k+1) r_c + i_{C1}(k)\left(\frac{T_s}{C} - r_c\right) \quad (23)$$

where VC1(k + 1) is the predicted capacitor voltage at the next sampling time and iC1(k) is capacitor current that depends on the states of the qZSI topology. According to the operational principle of qZS network explained in Section II-B, for nonshoot-through and shoot-through states, capacitor current can be defined as follows:

1) during nonshoot-through state

$$I_{C1} = I_{L1} - (S_a i_a + S_b i_b + S_c i_C) \quad (24)$$

2) during shoot-through state

$$i_{C1} = -I_{L1} \quad (25)$$

Cost function optimization

The selection of the cost function is a key part of the MPC scheme. The proposed MPC scheme has two cost functions, which are used to minimize output current and capacitor voltage errors in the next sampling time. The output current cost function is defined as

$$g_i = \left\| i_j^*(k+1) - i_j(k+1) \right\|^2 = [i_a^*(k+1) - i_a(k+1)]^2 + [i_b^*(k+1) - i_b(k+1)]^2 + [i_c^*(k+1) - i_c(k+1)]^2 \quad (26)$$

where i∗ j (k + 1) is the reference output current vector and ij(k + 1) is the predicted output current vector in the next step (j = a, b, c).

The cost function of capacitor voltage can also be defined as

$$g_v = \lambda * |v_{C1}^*(k+1) - v_{C1}(K+1)| \quad (27)$$

where v∗ C1(k + 1) and vC1(k + 1) are the reference and predicted capacitor voltages, respectively. The weighting factor (λ) was determined by using cost function classification technique that was detailed in [36]. The complete cost function is

$$g(k+1) = g_i(k+1) + g_v(k+1) \quad (28)$$

Control algorithm

The flowchart for the proposed control algorithm is given in Fig. 5.

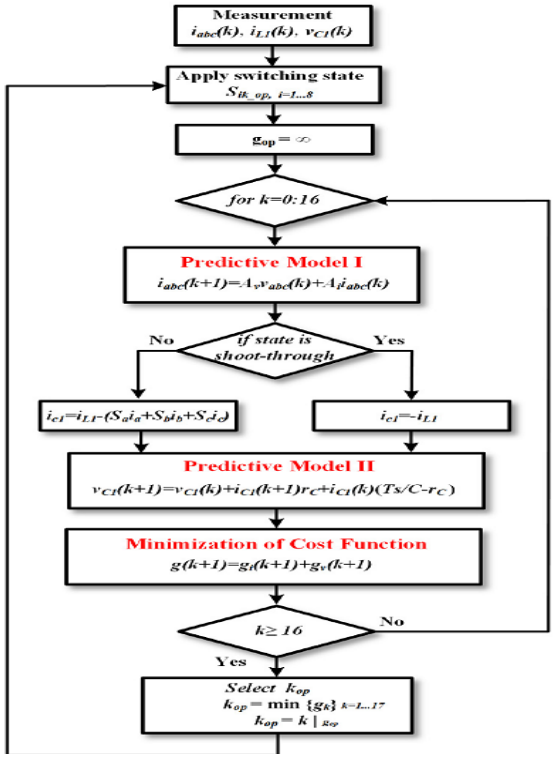

International Journal of Research
Available at https://edupediapublications.org/journals
e-ISSN: 2348-6848
p-ISSN: 2348-795X
Volume 04 Issue-17
December 2017

Fig. 5. Flowchart of the proposed MPC algorithm for qZS four-leg inverters

Cost function minimization is implemented as a repeated loop for each voltage vector to predict the values, evaluate the cost function, and store the minimum value and the index value of the corresponding switching state. The control algorithm can be summarized in the next steps.

1) Sampling the output phase currents (iabc), inductor current (iL1), and capacitor voltage (vC1).

Table I
Qzs four-leg inverter and load parameters

Parameter	Value
Input dc voltage (V_{in})	80–180 V
qZS network inductances (L_1, L_2)	2.5 mH
qZS network capacitors (C_1, C_2)	1000 μF
Load resistance	5–10 Ω
Filter inductance, L_f	10 mH
Filter resistance R_f	0.05 Ω
Nominal frequency (f_o)	50 Hz
Nominal output voltage (v_{ln})	50 V rms
Sampling time (T_s)	40 μs

2) These are used to predict output currents and capacitor voltage using the predictive model I, and II, respectively.

3) All predictions are evaluated using the cost function.

4) The optimal switching state that corresponds to the optimal voltage vector that minimizes the cost function is selected to be applied at the next sampling time.

PV SOURCE

Photovoltaics (PV) covers the conversion of light into electricity using semiconducting materials that exhibit the photovoltaic effect, a phenomenon studied in physics, photochemistry, and electrochemistry. The dynamic model of PV cell is shown in below Fig.6.

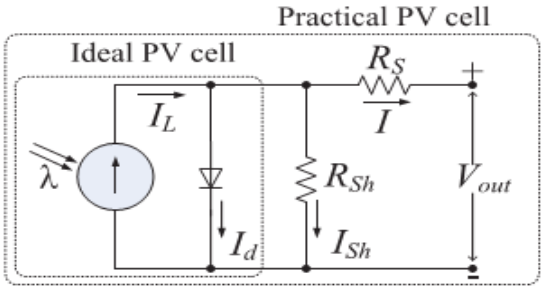

Fig 6.Equivalent electrical circuit of the PV cell.

The basic equation describing the I -V characteristic of a practical PV cell is

$$I = I_L - I_d - I_{sh} = I_L - I_D\left[e^{\frac{QV_{oc}}{AKT}-1}\right] - \frac{V_{out}+IR_S}{R_{Sh}} \quad (27)$$

where I D is the saturation current of the diode, Q is the electron charge, A is the curve fitting constant (or diode emission factor), K is the Boltzmann constant and T is the temperature on absolute scale. PV systems convert light directly into electricity and shouldn't be confused with other technologies, such as concentrated solar power or solar thermal, used for heating and cooling.

V SIMULATION RESULTS

To verify the theoretical analysis and confirm the proposed MPC technique of qZS four-leg inverter, simulation and experiments have been conducted with the configuration shown in Fig. 7. The parameters for both simulation and experiments are given in Table I.

Buck–boost conversion modes analysis

The proposed qZS four-leg inverter can operate both buck and boost conversion modes according to the input voltage and the desired output voltage.

Case-A1: Vin =180 V, M =0.8.

Simulation results of this case are shown in Fig. 7(a). Here, Vin >123 V, so qZSI works in buck conversion mode. Thus, the boost factor B = 1 and the voltage gain is G = B ·M = 0.8. The maximum output line-to-line voltage is

$$\hat{v}_{ab} = \hat{v}_{ab} = \hat{v}_{ab} = \sqrt{3}G.V_{in}/2 \cong 123V.$$

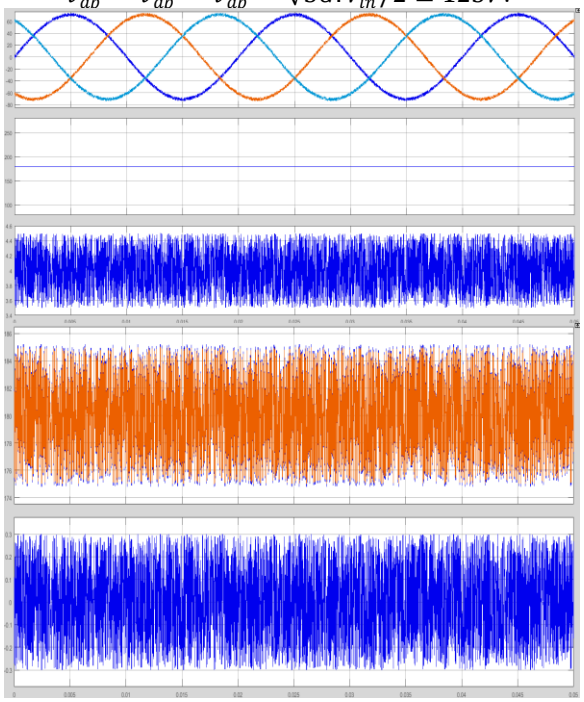

Fig. 7. Simulation results with the same output voltage at (a) Vin =180 V, M = 0.8; (b) Vin = 100 V, M = 1; and (c) Vin = 80 V, M = 0.85.

It can be observed from Fig. 6(a) that the voltage on C1 is equal to the input voltage 180 V and the voltage on C2 is 0 V. It can be noted that a pure dc current flows through an inductor due to the voltage on L1 is zero.

Fig. 7(c) shows the experimental results for this case. From (9), the boost factor B = 2.08 and the voltage gain G = 1.768 is obtained. Thus, the dc-link voltage (vPN) is boosted from 80 to 166 V. In this case, the maximum output line-to-line voltage is

$$\hat{V}_{ab} = \hat{V}_{bc} = \hat{V}_{ca} = \sqrt{3}.G.V_{in/2} \cong 123V$$

It can be seen from Fig. 6(c) that the voltage on C1 and C2 is 124 and 42 V, respectively. Experimental results show that the qZS four-leg inverter can provide constant output voltage under various input voltages without using dc/dc converter or transformer.

Case-A2:$V_{in} = 100V, M = 1$

In order to maintain constant output voltage, qZSI works in boost conversion mode because of Vin <123 V. The voltage on the dc link (vPN) is boosted from 100 to 142 V. In this case, the maximum output line-to-line voltage is

$$\hat{V}_{ab} = \hat{V}_{bc} = \hat{V}_{ca} = \sqrt{3}.G.V_{in/2} \cong 123V$$

It can be seen from Fig. 8(b) that the voltage on C1 and C2 is 120 and 22 V, respectively. Notice that the inductor current (iL1) is continuous that reduce the input stress. Case-A3: Vin =80 V, M =0.85.

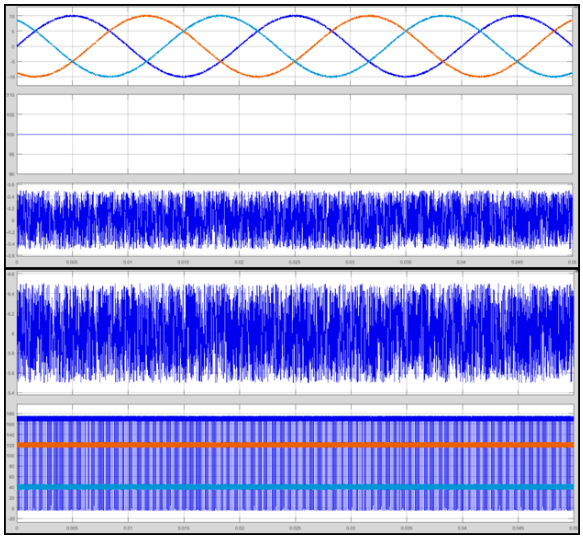

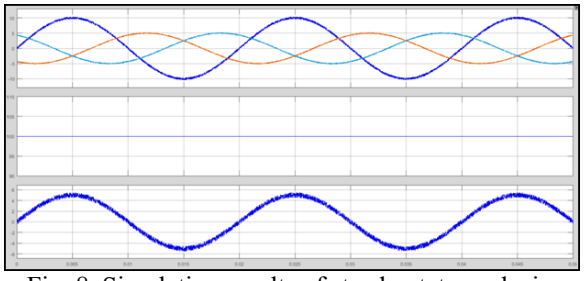

Fig. 8. Simulation results of steady-state analysis with (a) balanced reference currents and balanced loads; (b) balanced reference currents and unbalanced loads; and (c) unbalanced reference currents and balanced loads.

Steady-state analysis

To perform steady-state analysis, the reference of qZS network capacitor voltage (V ∗ c1) is set to 150 V and the input voltage is Vin=100 V, which results in the qZS four-leg inverter operating in boost mode in the following experimental studies.

The following three cases are considered to show the effectiveness of the proposed controller under steady-state operation.

1) Case-B1: Balanced reference currents (i∗ a = i∗ b = i∗ c = 10 A) and balanced loads (Ra = Rb = Rc = 7.5Ω).

2) Case-B2: Balanced reference currents (i∗ a = i∗ b = i∗ c = 10 A) and unbalanced loads (Ra = 5Ω, Rb = Rc = 7.5Ω).

3) Case-B3: Unbalanced reference currents (i∗ a = 10 A, i∗ b = 5 A, i∗ c = 5 A) and balanced loads (Ra = Rb = Rc = 10Ω).

Steady-state experimental results of these cases are shown in Fig. 7(a)–(c). All experimental results show that the output currents (ia, ib, ic) and the capacitor voltage (VC1) track their references (i∗ a, i∗ b, i∗ c, V ∗ C1) with high accuracy while the dc-link voltage (VPN) is kept constant. The neutral current, which is the sum of the three-phase load currents, is zero in cases of balanced reference current [see Fig. 8(a) and (b)]. On the other hand, the neutral current flows through the fourth leg of the inverter in case of the unbalanced reference current [see Fig. 8(c)].

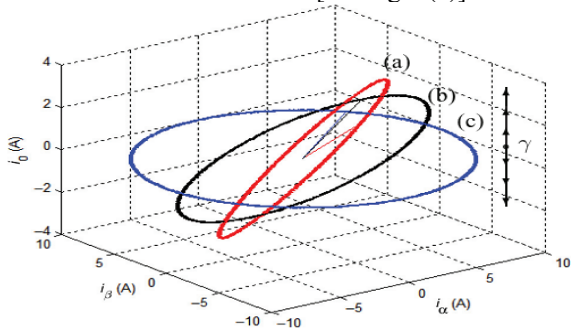

Fig. 9. Trajectories of output current under various reference currents (a) ia =10, ib =0 A, ic =10 A; (b) ia =10, ib =5 A, ic =5 A; and (c) ia = ib = ic =10 A.

The simulation result of the load currents trajectories under various reference values is shown in Fig. 8. The blue trace (c) is balanced current condition, while the black (b) and red (a) are unbalanced.

Transient-state analysis

The simulation results of transient-state analysis with balanced and unbalanced reference currents are shown in Fig. 10(a) and (b), respectively. The reference output currents step from 5 to 10 A are shown in Fig. 10(a).

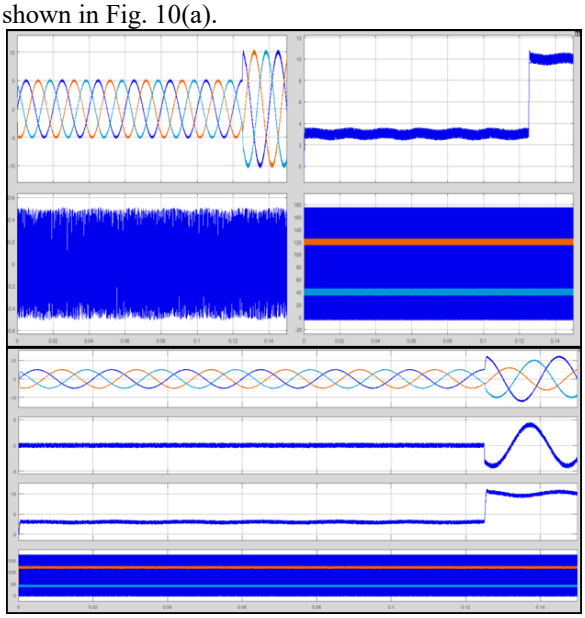

Fig. 10. Simulation results of transient-state analysis with (a) balanced reference currents and balanced loads and (b) unbalanced reference currents and balanced loads.

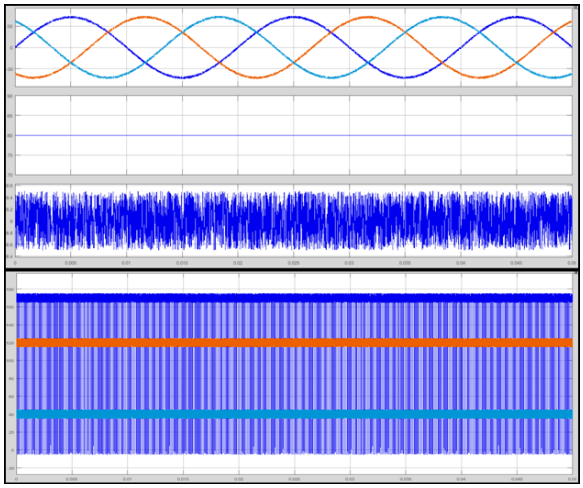

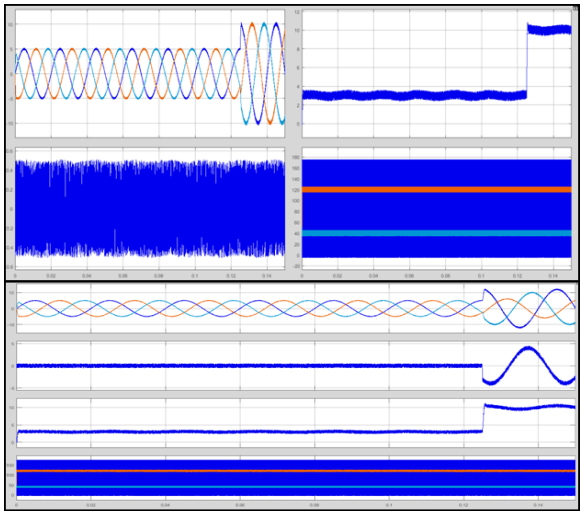

Fig. 11. Transient-state simulation results under single-phase open circuit fault. (a) Proposed qZS four-leg inverter. (b) Traditional qZS three leg inverter with MPC control.

Analysis of Symmetrical Components

To analyze the symmetrical components (zero, positive, and negative sequences) of the three-phase current signals under unbalanced conditions, Fortescue method is used [37]. The level of unbalance is also described by the negative sequence current unbalance factor (ρi), which is given as the modulus of the ratio of negative to positive sequence currents [same for the negative sequence voltage unbalance factor (ρv)].

$$\rho_i = \frac{i_n}{i_p} * 100\% \qquad (29)$$

where ip and in are the positive- and negative-sequence component, respectively.

Table II
Symmetrical components and unbalance factor

Case studies	i_0	i_p	i_n	ρ_i (%)
Fig. 7 (a): $i_a = i_b = i_c = 10$ A	0 A	10 A	0 A	0
Fig. 7 (c): $i_a = 10$ A, $i_b = i_c = 5$ A	1.67 A	6.67 A	1.67 A	25
Fig. 8 (a): $i_a = i_c = 10$ A, $i_b = 0$ A	3.33 A	6.67 A	3.33 A	50
Fig. 10 (b): $i_a = 7$ A, $i_b = 10$ A, $i_c = 12$ A	1.45 A	9.67 A	1.45 A	15

and their symmetrical components, and the negative sequence current unbalance factor. Phase angles of the currents are θa = 0◦, θb = −120◦, and θc = −240◦.

CONCLUSION

This paper has proposed an MPC scheme for qZS three phase four-leg inverter. Solar PV has specific advantages as an energy source: its operation generates no pollution and no greenhouse gas emissions once installed, it shows simple scalability in respect of power needs and silicon has large

availability in the Earth's crust. The main aim of this paper is to achieve single-stage power converter topology for renewable energy-based power generation systems under balanced and unbalanced conditions with high control capability. To do that, qZS three-phase four-leg inverter topology was proposed in this study. To improve control capability of the controller, the MPC scheme was employed in the controller stage. Simulation and experimental studies were performed to verify the performance of the proposed inverter topology and its control strategy. The results show that the proposed technique not only has an excellent steady-state and transient performances, but also it is robust against fault conditions.

REFERENCES

[1] H. Abu-Rub, M. Malinowski, and K. Al-Haddad, Power Electronics for Renewable Energy Systems, Transportation and Industrial Applications. Hoboken, NJ, USA: Wiley, 2014.
[2] X. Guo, D. Xu, and B. Wu, "Four-leg current-source inverter with a new space vector modulation for common-mode voltage suppression," IEEE Trans. Ind. Electron., vol. 62, no. 10, pp. 6003–6007, Oct. 2015.
[3] F. Z. Peng, "Z-source inverter," IEEE Trans. Ind. Appl., vol. 39, no. 2, pp. 504–510, Mar./Apr. 2003.
[4] S. Kouro, J. Leon, D. Vinnikov, and L. Franquelo, "Grid-connected photovoltaic systems: An overview of recent research and emerging PV converter technology," IEEE Ind. Electron. Mag., vol. 9, no. 1, pp. 47–61, Mar. 2015.
[5] Y. Li, S. Jiang, J. Cintron-Rivera, and F. Z. Peng, "Modeling and control of quasi-Z-source inverter for distributed generation applications," IEEE Trans. Ind. Electron., vol. 60, no. 4, pp. 1532–1541, Apr. 2013.
[6] B. Ge et al., "An energy-stored quasi-Z-source inverter for application to photovoltaic power system," IEEE Trans. Ind. Electron., vol. 60, no. 10, pp. 4468–4481, Oct. 2013.
[7] W. Qian, F. Z. Peng, and H. Cha, "Trans-Z-source inverters," IEEE Trans. Power Electron., vol. 26, no. 12, pp. 3453–3463, Dec. 2011.
[8] H. Jin, X. Rui, Z. Yunping, W. Zhi, and S. Haixia, "The study of SPWM control strategy to reduce common-mode interferences in threephase four-leg inverters," in Proc. 3rd IEEE Conf. Ind. Electron. Appl. (ICIEA'08), Jun. 2008, pp. 924–928.
[9] S. Bifaretti, A. Lidozzi, L. Solero, and F. Crescimbini, "Comparison of modulation techniques for active split dc-bus three-phase four-leg inverters," in Proc. IEEE Energy Convers. Congr. Expo. (ECCE), Sep. 2014, pp. 5631–5638.
[10] E. Demirkutlu and A. Hava, "A scalar resonant-filter-bank-based outputvoltage control method and a scalar minimum-switching-loss discontinuous PWM method for the four-leg-inverter-based three-phase four-wire power supply," IEEE Trans. Ind. Electron., vol. 45, no. 3, pp. 982–991, May 2009.
[11] Y. Liu, B. Ge, H. Abu-Rub, and F. Z. Peng, "An effective control method for three-phase quasi-Z-source cascaded multilevel inverter based grid-tie photovoltaic power system," IEEE Trans. Ind. Electron., vol. 61, no. 12, pp. 6794–6802, Dec. 2014.

E SHARADHA
Completed B.Tech in Electrical & Electronics Engineering in 2011 from JNTUH, HYDERABAD and Pursuing M.Tech from St. Martin's Engineering College, Dhullapally, Secunderabad, Telangana. Area of interest includes Power Electronics.
E-mail id: erragokula.sharada@gmail.com

D ARAVIND
Completed B.Tech in Electrical & Electronics Engineering from St. Martin's Engineering College and M.Tech in Power Electronics from CMR Engineering College and Technology, Hyderabad. Working as Assistant Professor in St. Martin's Engineering College, Dhullapally, Secunderabad, Telangana. Area of interest includes Power Electronics, FACTS Devices and Renewable Energy Sources.
E-mail id: aravind.smec204@gmail.com